Thin Films

International Edition: DOI: 10.1002/anie.201814034
German Edition: DOI: 10.1002/ange.201814034

Conductive Fused Porphyrin Tapes on Sensitive Substrates by a Chemical Vapor Deposition Approach

*Giuseppe Bengasi, Kamal Baba, Gilles Frache, Jessica Desport, Paul Gratia, Katja Heinze, and Nicolas D. Boscher**

Abstract: *Oxidative polymerization of nickel(II) 5,15-diphenyl porphyrin and nickel(II) 5,15-bis(di-3,5-tert-butylphenyl) porphyrin by oxidative chemical vapor deposition (oCVD) yields multiply fused porphyrin oligomers in thin film form. The oCVD technique enables one-step formation, deposition, and p-doping of conjugated poly(porphyrins) coatings without solvents or post-treatments. The decisive reactions and side reactions during the oCVD process are shown by high-resolution mass spectrometry. Owing to the highly conjugated structure of the fused tapes, the thin films exhibit an electrical conductivity of* $3.6\times10^{-2}\,S\,cm^{-1}$ *and strong absorption in the visible to near-infrared spectral region. The formation of smooth conjugated poly(porphyrins) coatings, even on sensitive substrates, is demonstrated by deposition and patterning on glass, silicon, and paper. Formation of conductive poly(porphyrins) thin films could enable the design of new optoelectronic devices using the oCVD approach.*

The exceptional properties of porphyrins are well-known in the scientific community, which has thoroughly investigated this class of compounds and its possible applications in functional devices such as solar cells,[1,2] sensors,[3,4] or catalysts.[5,6] The key features of interest of these compounds lay in their optical and optoelectronic properties that are intrinsically related to the chemical structure of the porphyrin macrocycle and its substituents. Similar to other compound classes,[7] the optical absorbance of porphyrins can be drastically shifted to the near-infrared (NIR) by conjugating the porphyrin core to further aromatic systems such as naphthalene.[8,9] Another way to obtain NIR absorbing porphyrins consists in the direct fusion of porphyrin rings. Osuka's group successfully demonstrated the formation of *meso-meso*/β-β/β-β triply fused porphyrin polymers using oxidative coupling reactions in solution. The very small band gaps of these tapes lead to absorptions in the NIR spectral region.[10] The most important fusion reaction employed zinc(II) porphyrins as monomers and silver(I) salts as oxidants, forming singly linked linear poly(porphyrins). Further oxidation using a combination of 2,3-dichloro-5,6-dicyano-1,4-benzoquinone and $Sc(OTf)_3$ increases the degree of conjugation.[11] Following these seminal works, the scientific community tried to improve the process employing different metalloporphyrins and more efficient oxidants enabling the formation of doubly or triply fused porphyrins in one-step reactions in solution.[12–16] Although these materials exhibit very interesting properties such as NIR and two-photon absorption, their very poor solubility and infusibility render their integration into devices very challenging or even impossible. To increase the solubility of directly fused porphyrins, solubilizing organic side chains were attached with the drawback of requiring tedious syntheses of the porphyrin monomers.[17] Bulky pendant groups, employed to prepare the bulk heterojunction blends, dilute the functional porphyrin macrocycle and hinder intermolecular π–π stacking, yielding relatively poor photovoltaic performances.[18] Furthermore, the solution-based approaches developed so far are limited to a small range of suitable substrates restricting possible applications of directly fused porphyrins. Several studies have also reported the formation of fused porphyrins from the sublimation under ultra-high vacuum onto oriented metal surfaces, for example, Ag(111),[19] or their fusion with graphene nanostructures.[20] However, in the latter approaches, the direct coupling of porphyrins at a surface is fully dependent on the supporting substrate.

Oxidative chemical vapor deposition (oCVD) is an elegant method for the simultaneous synthesis and deposition of conjugated polymer thin films on a wide variety of substrates.[21] oCVD relies on the vapor phase delivery of a monomer and an oxidant to a surface. Conjugated doped polymers then form directly on the substrate. The technique is successfully used for the production of doped poly(3,4-ethylenedioxythiophene) (PEDOT)[22] or polyaniline thin films from the respective thiophene and aniline monomers.[23] To date, oCVD involves chemically rather simple monomers such as pyrroles, thiophenes, or selenophenes. Yet, these monomers alone are incompetent to confer highly advanced optical and optoelectronic properties to the obtained thin films.

[*] G. Bengasi, Dr. K. Baba, Dr. G. Frache, Dr. J. Desport, Dr. P. Gratia, Dr. N. D. Boscher
Materials Research and Technology
Luxembourg Institute of Science and Technology (LIST)
5 Avenue des Hauts-Fourneaux, 4362 Esch/Alzette (Luxembourg)
E-mail: nicolas.boscher@list.lu
G. Bengasi, Prof. Dr. K. Heinze
Institute of Inorganic Chemistry and Analytical Chemistry
Johannes Gutenberg University of Mainz
Duesbergweg 10–14, 55128 Mainz (Germany)
Supporting information and the ORCID identification number(s) for the author(s) of this article can be found under: https://doi.org/10.1002/anie.201814034.

Herein we report the simultaneous synthesis, deposition, and p-doping of fused porphyrin thin films by an oCVD approach. As specific functionalization of the porphyrin monomer is not required, commercially available or easy-to-prepare inexpensive porphyrins are employed. The oxidative polymerization of these porphyrins is evidenced by ultraviolet-visible-near infrared (UV/Vis-NIR) spectroscopy, laser desorption ionization high-resolution mass spectrometry (LDI-HRMS), and gel permeation chromatography (GPC). Our study corroborates the decisive C–C bond-forming reactions and side reactions occurring during the oCVD reaction of porphyrins. The morphology of the fused porphyrin thin films is assessed by scanning electron microscopy (SEM) and atomic force microscopy (AFM). The electrical properties of the resulting fused porphyrin thin films are evaluated by conductivity measurements. Finally, the oCVD approach is used to form patterned conductive fused porphyrin thin films on a variety of substrates, namely silicon, glass, and printer paper.

Based on its hydrolytic stability even in the presence of acids formed in the oxidative polymerization process and the availability of unsubstituted *meso* and β positions for polymerization, we selected nickel(II) 5,15-diphenyl porphyrin (NiDPP) as suitable monomer for oCVD (Scheme 1). As

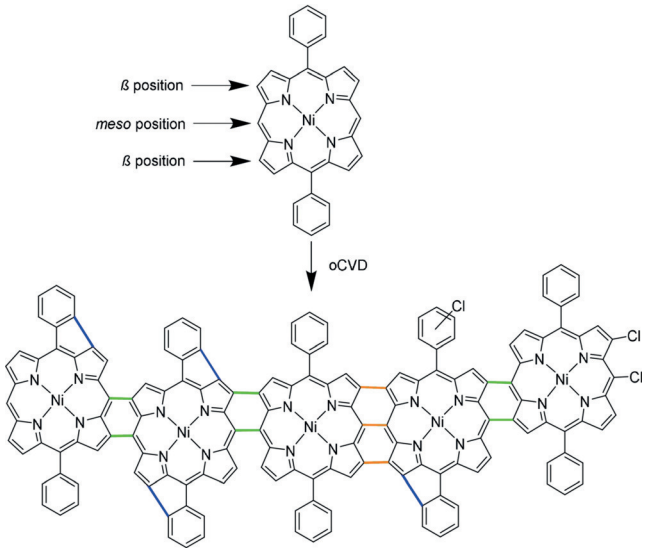

Scheme 1. The oxidative coupling reaction of NiDPP with $FeCl_3$. The reaction leads to coupling of the monomers thanks to the unsubstituted *meso* and β positions of NiDPP. NiDPP allows formation of β-*meso* bonds (green bonds) and β-*meso*-β triply linked porphyrin units (orange bonds). Chlorination is observed but the reactive site is not identified and only example positions are depicted. Blue bonds indicate a possible intramolecular cyclization between the phenyl substituent and a pyrrole.

oxidant we chose iron(III) chloride owing to its proven high suitability for oCVD processes[24] and owing to the ability of Fe^{3+} species to promote the synthesis of directly fused porphyrins in solution chemistry approaches.[12] The oCVD reaction was performed under reduced pressure (10^{-3} mbar) in a customized stainless steel reaction chamber equipped with two crucibles used to simultaneously sublime NiDPP

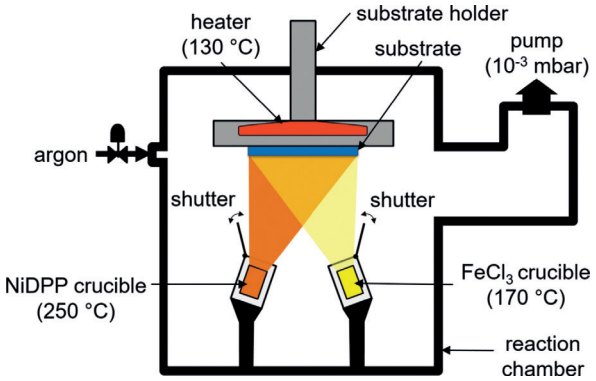

Figure 1. The oCVD reactor. The heated substrate is placed above two heated crucibles containing the oxidant and the metalloporphyrin, respectively. The pressure of the chamber is reduced to 10^{-3} mbar to ensure sublimation of the monomers and oxidants at reasonable temperatures.

(250 °C) and $FeCl_3$ (170 °C) (Figure 1). Printer paper sheets, microscope glass slides, silicon wafers, and commercial organic field-effect transistor chips were used as substrates to demonstrate the versatility and potential of the oCVD approach. The substrates were placed on a heated stage placed 20 cm above the two crucibles. The oCVD reaction of NiDPP with $FeCl_3$ yields 200 nm thick and strongly colored dark green coatings. Such a dark green coloration contrasts with the orange color of the reference NiDPP coating prepared from the sublimation of NiDPP in the absence of an oxidant (Figure 2).

Figure 2. Optical image of the sublimed NiDPP coating (orange, left) and patterned oCVD NiDPP coating (green, right) deposited on paper. The green oCVD NiDPP coating displays electrical conductivity.

UV/Vis-NIR spectroscopic analysis, performed on coated glass substrates, reveals significant differences in the absorption spectrum of the dark green oCVD NiDPP coating with respect to the orange sublimed NiDPP coating. The absorption around 360 nm increases, the Soret band broadens, the red-shifted Q bands collapse to a new broad band around 668 nm and, importantly, broad absorptions appear in the NIR region up to 2200 nm (Figure 3). These observations are in full agreement with the formation of multiply fused porphyrins that typically exhibit broad absorptions that can reach the NIR spectral region, while singly linked porphyrins only yield absorption in the UV/Vis region.[14,17]

In contrast to the soluble sublimed NiDPP coating, the oCVD NiDPP coating is almost insoluble in common organic

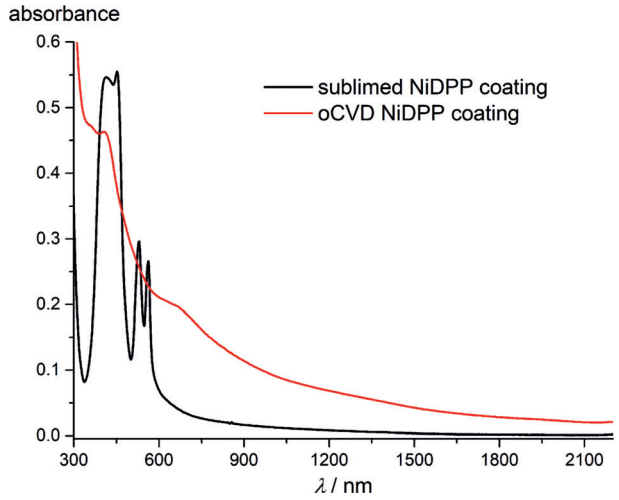

Figure 3. Comparison of the UV/Vis-NIR absorption spectra of the sublimed (black) and oCVD (red) NiDPP coatings formed on glass substrates.

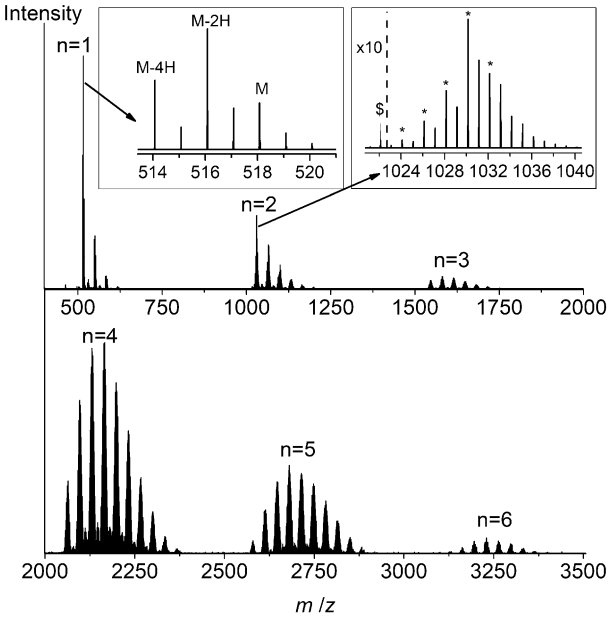

Figure 4. LDI-HRMS spectra of the oCVD NiDPP coating. The spectra reveal the presence of monomeric to hexameric species ($n=1$–6) and peak distributions owing to exchange of hydrogen by chlorine atoms deriving from the oxidant. The left inset shows the loss of hydrogens likely due to an intramolecular cyclization reaction ($n=1$). The same reaction occurs in the dimer region ($n=2$), where the signals overlap with the isobaric formation of new bonds between the monomeric units (right inset, "*"). The spectrum shows the presence of a triply linked porphyrin dimer with four phenyl rings fused on the porphyrin core ("$").

solvents such as THF, acetone, dichloromethane, or hexafluoroisopropanol (Supporting Information, Figure S1). UV/Vis-NIR analysis of the acetone-soluble phase ascertains the presence of unreacted $FeCl_3$ and NiDPP monomer derivatives (Supporting Information, Figure S2). Although red-shifted, the Soret and Q bands still appear clearly in the absorption spectrum of the acetone solution. This indicates that the porphyrin core is essentially intact, yet reactions able to modify the HOMO–LUMO gap of the porphyrin must have occurred. Compared to the pristine NiDPP monomer, the number of the Q bands increased in the soluble part of the oCVD NiDPP coating pointing to a different symmetry of some macrocyclic species (Supporting Information, Figure S3). This spectral evidence, along with the partial solubility of the oCVD NiDPP coating, confirm the presence of a variety of chain lengths that yield both soluble and insoluble fractions and side reactions that modify the porphyrin symmetry. However, the absence of NIR absorption in the soluble fraction of the oCVD NiDPP coating suggests that the highly conjugated poly(porphyrins) are insoluble and stick to the glass substrate even upon rinsing.

The relative atomic compositions of the oCVD NiDPP coating, obtained by XPS, are rather close to the theoretical ones of NiDPP and fused NiDPP oligomers (Supporting Information, Table S1). The slight decrease of the nickel, nitrogen, and carbon element concentrations is associated to the expected incorporation of iron (3%) and chlorine (2%) into the oCVD NiDPP coating. Analysis of the Cl 1s XPS spectrum reveals the presence of two chlorine environments. The first contribution at lower binding energies is associated to residues of unreacted $FeCl_3$ or $FeCl_2$ by-products in the oCVD NiDPP coating (Supporting Information, Figure S4). The second chlorine environment at higher binding energies is attributed to organic chloride, most probably related to the chlorination of the porphyrin macrocycles, which is a well-known side reaction when fusing porphyrins in presence of $FeCl_3$.[8]

LDI-HRMS analysis directly acquired from the oCVD NiDPP coating reveals the presence of NiDPP oligomers confirming the successful oxidative polymerization of NiDPP (Figure 4). The signal related to the presence of the free-base porphyrin H_2DPP is negligibly weak, confirming that NiDPP effectively retains the nickel ion in the porphyrin core during the deposition and polymerization. Up to hexameric oligomers are observed in the mass spectrum (Figure 4), which corresponds to the instrumental limit (4000 m/z). Although LDI-HRMS analysis does not provide an exhaustive view into the mass distribution and the intensities related to the different species detected are not directly related to their abundance, the high resolution of the technique (up to 0.003 amu) represents a valuable tool for the unambiguous characterization of the sample. Moreover, the formation of even longer oligomers, with masses outside the instrumental limit, is conceivable. Unfortunately, the insolubility of the oCVD NiDPP coating prohibits GPC analysis and consequently the detailed mass distribution of the oCVD NiDPP coating remains elusive. Nonetheless, the absorptions up to 2200 nm in the UV/Vis-NIR absorption spectrum (Figure 3) strongly suggest the presence of highly conjugated poly(porphyrins), since singly linked porphyrins are NIR-transparent.[25]

With the aim to perform a GPC analysis and undoubtedly demonstrate the direct fusion of porphyrin in oCVD, we investigated the oCVD reaction of nickel(II) 5,15-bis(di-3,5-*tert*-butylphenyl) porphyrin (NiDD*t*-BuPP). The introduction

of the *tert*-butyl groups to the pendant phenyl substituents should reduce the intermolecular π–π stacking and ensure a better solubility of the formed fused porphyrins.[26] Moreover, with the aim to produce shorter and THF-soluble fused porphyrin oligomers that can be characterized by GPC, a lower temperature (150 °C) was employed to sublimate the oxidant limiting the oxidant delivered to the substrate. The UV/Vis-NIR (Supporting Information, Figure S5) and LDI-HRMS spectra (Supporting Information, Figure S6) of the oCVD NiDD*t*-BuPP coating evidence a highly similar behaviour between NiDD*t*-BuPP and NiDPP with an absorbance in the NIR region and the detection of multiply fused oligomers. Furthermore, the structure and deposition conditions of the oCVD NiDD*t*-BuPP coating allows its GPC analysis. The GPC analysis of the oCVD NiDD*t*-BuPP coating confirms the formation of polymeric species (Supporting Information, Figure S7). UV detection confirms the presence of monomeric units together with a broad polymer distribution, exhibiting masses up to 5000 g mol^{-1} (relative to polystyrene standards), in good agreement with LDI-HRMS data. The far lower solubility of the NiDPP oCVD coating and its oligomers intensities ratio in the LDI-HRMS spectra suggest that NiDPP could possess an even higher chain length.

The mass spectrometric analysis of the two oCVD NiDD*t*-BuPP and oCVD NiDPP coatings confirms the formation of one to three C–C bonds between the porphyrin units (Scheme 1). The LDI-HRMS spectra display signals related to the formation of triply linked β-β/*meso*-*meso*/β-β porphyrins for NiDPP (Figure 4). This is in contrast to solution-based oxidative polymerization processes delivering only double *meso*-β/*meso*-β linkages between the porphyrin units.[14,27] LDI-HRMS reveals another unexpected difference between the oCVD approach and the reported solution-based methods. For the peak distributions related to both the porphyrin monomer and oligomers, the LDI-HRMS spectrum exhibits signals suggesting the simultaneous elimination of two hydrogen atoms 2H (Figure 4; Supporting Information, Figure S6). Since the maximum number of hydrogen pairs eliminated is proportional to the number of phenyl rings in the detected monomeric and oligomeric species, we attribute these signals to dehydrogenated species. As a hypothesis, we suggest that these species could have formed by intramolecular cyclization reactions between the phenyl substituents and the porphyrin pyrrole *β* positions. Possibly, this intra-porphyrin dehydrogenation could also assist in the formation of triply linked porphyrins, since porphyrin π extension via ring fusion should modify the electron distribution and the reactivity of the porphyrin *β* positions towards the oxidative coupling.

Furthermore, the LDI-HRMS spectra exhibits peak distributions showing multiple chlorine incorporation. In fact, the distance between the peaks equals the exchange of a hydrogen atom by chlorine. Partial chlorination could also account for the very low solubility of the present oCVD NiDPP coating, since chlorination is known to decrease porphyrin solubility.[28] Both these side reactions are related to the use of $FeCl_3$ as oxidant, as $FeCl_3$ is competent to cause chlorination of porphyrins (especially in presence of Cl_2 that could be produced during the sublimation of the oxidant) and cyclization of aromatic rings on the porphyrin core.[8,29,30] Furthermore, both chlorination and extension of the π conjugation owing to the phenyl cyclization should modify the HOMO–LUMO gaps and modify the orbital symmetry. This is in agreement with the LDI-HRMS analysis of the poorly soluble fraction of oCVD NiDPP coating in acetone that confirms the presence of chlorinated and dehydrogenated compounds (Supporting Information, Figure S8).

Since we expected fused porphyrins being electrically conductive, basic charge transport properties of the oCVD NiDPP and oCVD NiDD*t*-BuPP coatings were investigated. The electrical conductivity of the oCVD coatings deposited onto commercial OFET chips was measured without applying any gate voltage and recording the current–voltage scans with a two-point probe to extract the conductivity using Ohm's law. Gratifyingly, the oCVD NiDPP coating displays an electrical ohmic conductivity with a value of 3.6×10^{-2} S cm^{-1} (Figure 5c). Although the obtained value is several orders of magnitude lower than the record reported for oCVD synthesized PEDOT films (6300 S cm^{-1}),[31] such a conductivity value is outstanding for a poly(porphyrin) thin film and may be useful for organic photonic and optoelectronic applications. Moreover, the room for improvement is vast since no optimization of the process was performed so far. The measured conductivity suggests that the oCVD NiDPP coating is a p-doped semiconducting material owing to the

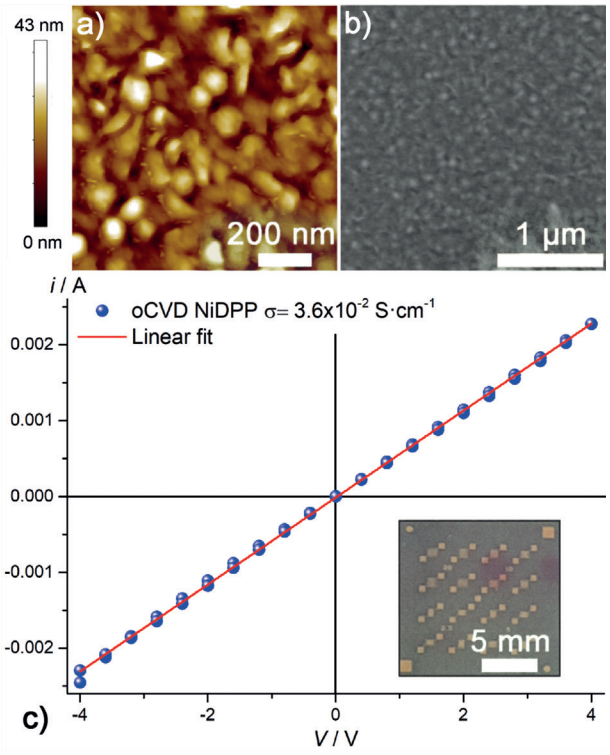

Figure 5. a) Atomic force microscopy and b) scanning electron microscopy images of a 200 nm thick oCVD NiDPP coating deposited on a silicon wafer. c) Lateral electrical conductivity measurement of the oCVD NiDPP coating deposited on OFET chips used to determine the conductivity (inset).

excess of $FeCl_3$ that is known to act as doping agent during the oCVD process.[22] Unfortunately, determining the hole mobility via field-effect measurements was impossible owing to the high conductivity of the oCVD NiDPP coating (p-doped), which results in the channel being ON already at zero gate voltage. Interestingly, the oCVD NiDD*t*-BuPP coating, polymerized from a reduced amount of $FeCl_3$ compared to the oCVD NiDPP coating, exhibits a drastically reduced conductivity (2.5×10^{-7} S cm^{-1}; Supporting Information, Figure S9). The large discrepancy between the conductivity of the oCVD NiDPP and oCVD NiDD*t*-BuPP coatings likely arises from 1) the presumably lower polymerisation length of the fused NiDD*t*-BuPP oligomers and 2) the reduced dopant concentration due to the lower oxidant reactant amount employed for in the oCVD reaction as well as from 3) a reduced intermolecular π–π stacking of the oligomers in the oCVD NiDD*t*-BuPP coatings. The reduction of the intermolecular π–π stacking by bulky substituents is a strong limitation to the photovoltaic performances of fused porphyrins.[18] Thus, the ability to directly fused porphyrins irrespective of their substituents should rapidly improve the photovoltaic performances of these visible-NIR light absorbent materials.

Finally, to demonstrate the potential of the oCVD of porphyrins for direct integration of conjugated poly(porphyrins) into optoelectronic devices, such as LEDs or hole-transporting materials in solar cells, we employed masks to coat and pattern various substrates. In particular, we readily deposited the oCVD NiDPP coating on printer paper using masks (Figure 2). The patterned film perfectly resembles the used mask with conjugated poly(porphyrin) lines as thin as one millimetre. Interestingly, electrical conductivity was even observed for the oCVD NiDPP coating deposited on printer paper. Scanning electron microscopy (SEM) and atomic force microscopy (AFM) analyses made on a 200 nm thick oCVD NiDPP coating deposited on a silicon wafer reveal the formation of a rather smooth (Sa = 4.6 nm) granular morphology composed of ca. 50 nm particles (Figure 5 a,b). The oCVD NiDPP coating is only slightly rougher that its sublimed counterpart (Supporting Information, Figures S10, S11). The ability to readily synthesize fused porphyrins and deposit them as smooth and dense thickness-controlled thin films represent a breakthrough in a field limited so far by low synthetic yields and the impossibility to process the produced materials in thin film form. The exceptional porphyrin and fused-porphyrin functionalities coupled to a substrate independent CVD approach suitable for patterning offers many strong advantages in the design of devices, including solar cells,[18] multi-charge storage systems,[32] sensors, and catalytic[33] and photocatalytic systems.[34]

In summary, the one-step synthesis, deposition and doping of multiply fused porphyrin oligomers, was achieved from a substrate independent and up-scalable oxidative chemical vapor deposition approach using simple metalloporphyrins and inexpensive oxidants. The oCVD reaction of NiDD*t*-BuPP yields up to pentamers for the investigated reaction conditions. On the other hand, the oCVD reaction of NiDPP likely forms slightly longer oligomers as assumed from the large increase of the conductivity. However, the insolubility of the oCVD NiDPP coating prevents GPC analysis and the limited range of observation of LDI-HRMS (up to NiDPP hexamers detected) does not allow to assess any polymerization length. Along the targeted oxidative polymerization of porphyrins, two side reactions, namely porphyrin chlorination and porphyrin π extension via intramolecular ring fusion, occur in the oCVD process. These side reactions, which initially might be seen as limitations of the oCVD process, may also be used as an asset to 1) decrease the solubility of the formed conjugated poly(porphyrins) and hence to stabilize the film and to 2) further increase the π conjugation. Further studies to gain a deeper understanding on the role of the metal center of the porphyrin, of the porphyrin substituents, and of the employed oxidant are currently ongoing in our laboratories. Finally, oCVD allowed the deposition of the conjugated poly(porphyrins) as thin films that can be exploited for the fabrication of optoelectronic devices thanks to the high electrical conductivity of the oCVD NiDPP coating of 3.6×10^{-2} S cm^{-1}. The versatility of this approach and its ability to pattern and deposit conjugated poly(porphyrins) thin films on sensitive and flexible substrates, such as paper, may pave the way to a plethora of future applications.

Acknowledgements

We gratefully acknowledge the financial support of the Luxembourg National Research Fund (fnr.lu) through the POLYPORPH project (C15/MS/10340560/POLYPORH/Boscher). D. El Assad, J. L. Biagi, Dr. J. Guillot, and P. Grysan from LIST are acknowledged for data collection and insightful discussions. We thank M. Gerard from LIST for the design and development of the oCVD reactor.

Conflict of interest

The authors declare no conflict of interest.

Keywords: chemical vapor deposition · oxidative coupling · polymerization · porphyrins · thin films

How to cite: *Angew. Chem. Int. Ed.* **2019**, *58*, 2103–2108
Angew. Chem. **2019**, *131*, 2125–2130

[1] S. Mathew, A. Yella, P. Gao, R. Humphry-Baker, B. F. E. Curchod, N. Ashari-Astani, I. Tavernelli, U. Rothlisberger, M. K. Nazeeruddin, M. Grätzel, *Nat. Chem.* **2014**, *6*, 242–247.
[2] L.-L. Li, E. Wei-Guang Diau, *Chem. Soc. Rev.* **2013**, *42*, 291–304.
[3] C. H. A. Esteves, B. A. Iglesias, R. W. C. Li, T. Ogawa, K. Araki, J. Gruber, *Sens. Actuators B* **2014**, *193*, 136–141.
[4] P. Heier, N. D. Boscher, T. Bohn, K. Heinze, P. Choquet, *J. Mater. Chem. A* **2014**, *2*, 1560–1570.
[5] K. Rybicka-Jasińska, W. Shan, K. Zawada, K. M. Kadish, D. Gryko, *J. Am. Chem. Soc.* **2016**, *138*, 15451–15458.
[6] S. Lin, C. S. Diercks, Y.-B. Zhang, N. Kornienko, E. M. Nichols, Y. Zhao, A. R. Paris, D. Kim, P. Yang, O. M. Yaghi, C. J. Chang, *Science* **2015**, *349*, 1208–1213.

[7] Y. Jiang, X. Zheng, Y. Deng, H. Tian, J. Ding, Z. Xie, Y. Geng, F. Wang, *Angew. Chem. Int. Ed.* **2018**, *57*, 10283 – 10287; *Angew. Chem.* **2018**, *130*, 10440 – 10444.
[8] J. P. Lewtak, D. Gryko, D. Bao, E. Sebai, O. Vakuliuk, M. Ścigaj, D. T. Gryko, *Org. Biomol. Chem.* **2011**, *9*, 8178 – 8181.
[9] L. Dou, Y. Liu, Z. Hong, G. Li, Y. Yang, *Chem. Rev.* **2015**, *115*, 12633 – 12665.
[10] A. Tsuda, A. Osuka, *Adv. Mater.* **2002**, *14*, 75 – 79.
[11] A. Tsuda, A. Osuka, *Science* **2001**, *293*, 79 – 82.
[12] C.-M. Feng, Y.-Z. Zhu, S.-C. Zhang, Y. Zang, J.-Y. Zheng, *Org. Biomol. Chem.* **2015**, *13*, 2566 – 2569.
[13] B. J. Brennan, M. J. Kenney, P. A. Liddell, B. R. Cherry, J. Li, A. L. Moore, T. A. Moore, D. Gust, *Chem. Commun.* **2011**, *47*, 10034 – 10036.
[14] A. Tsuda, Y. Nakamura, A. Osuka, *Chem. Commun.* **2003**, 1096 – 1097.
[15] B. J. Brennan, J. Arero, P. A. Liddell, T. A. Moore, A. L. Moore, D. Gust, *J. Porphyrins Phthalocyanines* **2013**, *17*, 247 – 251.
[16] A. A. Ryan, M. O. Senge, *Eur. J. Org. Chem.* **2013**, 3700 – 3711.
[17] N. Yoshida, N. Aratani, A. Osuka, *Chem. Commun.* **2000**, 197 – 198.
[18] J. Kesters, P. Verstappen, M. Kelchtermans, L. Lutsen, D. Vanderzande, W. Maes, *Adv. Energy Mater.* **2015**, *5*, 1500218.
[19] A. Wiengarten, K. Seufert, W. Auwärter, D. Ecija, K. Diller, F. Allegretti, F. Bischo, S. Fischer, D. A. Duncan, A. C. Papageorgiou, et al., *J. Am. Chem. Soc.* **2014**, *136*, 9346 – 9354.
[20] Y. He, M. Garnica, F. Bischoff, J. Ducke, M. Bocquet, M. Batzill, W. Auwärter, J. V. Barth, *Nat. Chem.* **2016**, *9*, 33 – 38.
[21] M. Wang, X. Wang, P. Moni, A. Liu, D. H. Kim, W. J. Jo, H. Sojoudi, K. K. Gleason, *Adv. Mater.* **2017**, *29*, 1604606.
[22] W. E. Tenhaeff, K. K. Gleason, *Adv. Funct. Mater.* **2008**, *18*, 979 – 992.
[23] Y. Y. Smolin, M. Soroush, K. K. S. Lau, *Beilstein J. Nanotechnol.* **2017**, *8*, 1266 – 1276.
[24] H. Goktas, X. Wang, N. D. Boscher, S. Torosian, K. K. Gleason, *J. Mater. Chem. C* **2016**, *4*, 3403 – 3414.
[25] A. Osuka, H. Shimidzu, *Angew. Chem. Int. Ed. Engl.* **1997**, *36*, 135 – 137; *Angew. Chem.* **1997**, *109*, 93 – 95.
[26] T. Tanaka, A. Osuka, *Chem. Soc. Rev.* **2015**, *44*, 943 – 969.
[27] A. Tsuda, A. Nakano, H. Furuta, H. Yamochi, A. Osuka, *Angew. Chem. Int. Ed.* **2000**, *39*, 558 – 561; *Angew. Chem.* **2000**, *112*, 572 – 575.
[28] M. O. Senge, O. Flögel, K. Ruhlandt-Senge, *J. Porphyrins Phthalocyanines* **2001**, *5*, 503 – 506.
[29] T. Wijesekera, A. Matsumoto, D. Dolphin, D. Lexa, *Angew. Chem. Int. Ed. Engl.* **1990**, *29*, 1028 – 1030; *Angew. Chem.* **1990**, *102*, 1073 – 1074.
[30] L. E. Wilson, N. W. Gregory, *J. Phys. Chem.* **1958**, *62*, 433 – 437.
[31] X. Wang, X. Zhang, L. Sun, D. Lee, S. Lee, M. Wang, J. Zhao, Y. Shao-horn, M. Dinc, T. Palacios, K. K. Gleason, *Sci. Adv.* **2018**, *4*, eaat5780.
[32] D. Bonifazi, M. Scholl, F. Song, L. Echegoyen, G. Accorsi, N. Armaroli, *Angew. Chem. Int. Ed.* **2003**, *42*, 4966 – 4970; *Angew. Chem.* **2003**, *115*, 5116 – 5120.
[33] D. Khusnutdinova, B. L. Wadsworth, M. Flores, A. M. Beiler, E. A. R. Cruz, Y. Zenkov, G. F. Moore, *ACS Catal.* **2018**, *8*, 9888 – 9898.
[34] A. Fateeva, P. A. Chater, C. P. Ireland, A. A. Tahir, Y. Z. Khimyak, P. V. Wiper, J. R. Darwent, M. J. Rosseinsky, *Angew. Chem. Int. Ed.* **2012**, *51*, 7440 – 7444; *Angew. Chem.* **2012**, *124*, 7558 – 7562.

Manuscript received: December 10, 2018
Accepted manuscript online: December 17, 2018
Version of record online: January 21, 2019

